$W^{\pm}$ and Z^0 polarization in pair production: Dominant helicities

C. L. Bilchak and R. W. Brown
Physics Department, Case Western Reserve University, Cleveland, Ohio 44106

J. D. Stroughair
Department of Theoretical Physics, Manchester University, Manchester M13 9PL, United Kingdom
(Received 3 June 1983)

We analyze the angular distributions and polarization that are expected for Drell-Yan or e^+e^- annihilation into boson pairs such as $W\gamma$ and WW. A helicity rule is formulated in renormalizable theories for massive-boson bremsstrahlung by a lepton or quark, relating the handedness of the boson to that of the fermion. The polarization for single-boson production in various reactions is also compared to this rule. A covariant W polarization basis is introduced in conjunction with the radiation representation for $W\gamma$ production.

I. INTRODUCTION

With the putative discovery[1] of the weak bosons $W^{\pm}$ and Z^0 in $p\bar{p}$ collisions, it remains to be verified that such particles have all the requisite gauge properties predicted by the Glashow-Weinberg-Salam $SU_L(2)\times U(1)$ (GWS) electroweak theory. Already the masses implied by the data are in excellent agreement with the standard predictions,[2]

$$M_W \cong 82\pm 2.4\ \text{GeV}/c^2\ , \qquad M_Z \cong 94\pm 2.0\ \text{GeV}/c^2\ , \tag{1.1}$$

for

$$\sin^2\theta_W \cong 0.23\pm 0.01\ . \tag{1.2}$$

(In the calculations described in our paper, we take $M_W=80\ \text{GeV}/c^2$, $M_Z=90\ \text{GeV}/c^2$, $\sin^2\theta_W=0.23$.) The production rate of decay leptons also agrees well with the theoretical estimates[3] based on the Drell-Yan mechanism.

Experimental attention now is focused on the decay spectra. The energy and angular decay distributions that are sensitive to the forms of the boson couplings can be compared to the GWS predictions.

In order to analyze the decay, it is necessary to know the average spin state of the W and Z in the relevant reference frame. Our paper addresses this question,[4] particularly in the production of electroweak pairs ($W\gamma, WW, WZ$, etc.) where the boson trilinear self-couplings come into play. We consider both quark-antiquark annihilation apropos of $p\bar{p}$ and pp collisions and e^+e^- annihilation, asking how the boson polarizations, as a function of angle and energy, change when the couplings are changed.

With this polarization information we can also compare the results to helicity rules in quantum electrodynamics (QED). The interesting theoretical question is the extent to which renormalizable electroweak physics imitates its QED subset. Of course, renormalizability implies that the longitudinal polarization for bosons with mass is controlled in the high-energy limit.

It is instructive to review first (Sec. II) the annihilation channel $e^+e^-\to\gamma\gamma$, since the polarization of other boson pairs, in both e^+e^- and proton colliders, has a close parallel to this QED reaction. The polarization (energy and angular dependences) of boson pairs in which one boson is the photon or the gluon is discussed in Sec. III: $e^+e^-\to Z\gamma$; $q\bar{q}'\to W\gamma, Z\gamma, Wg, Zg$. The cases where both are weak bosons are considered in Sec. IV: $e^+e^-\to WW, ZZ$; $q\bar{q}'\to WW, WZ, ZZ$. Comparisons are made with nonrenormalizable couplings.

We also compare the polarization expected for single production in Sec. V, including the seminal $q\bar{q}'\to W, Z$ quark annihilation and the related decay-lepton asymmetry. The neutrino-induced reaction $\nu_l N\to WlX$ and analogous single-boson production in e^+e^- and ep, although somewhat academic at this point, complete the theoretical picture.

The analytic demonstration of a handedness-matching rule that emerges from our numerical survey is the subject of Sec. VI where a covariant W polarization basis and the so-called radiation representation are utilized. In those reactions where forward boson emission by a hard fermion is dominant, the survey shows the strong tendency of the boson to follow the fermion handedness, a fact that is useful quantitatively as well as qualitatively and is summarized in terms of "hemispheres" in Sec. VII. We define the parent hemisphere to be the forward (2π solid angle) hemisphere into which the parent is moving, with the equatorial plane perpendicular to its initial motion. The rule thus describes that situation where the emitted boson has the same handedness as the parent, when it is emitted into the parent's hemisphere.

II. PHOTON POLARIZATION IN $f\bar{f}\to\gamma\gamma$: A REVIEW

The polarization results to be discussed in the next two sections are closely related to the lowest-order Dirac-fermion—antifermion annihilation into photon pairs,

$$f\bar{f}\to\gamma\gamma\ , \tag{2.1}$$

the diagrams for which appear in Fig. 1(a). The differential cross section for (2.1) and for a given photon polarization is carried out by adapting the weak-boson calculations pertinent to the next section; we refer the reader to Sec. III for their description. Specific fermion helicities are chosen for the illustration. At energies far above the fermion mass, the fermion helicity is well known to be preserved along the fermion line in QED. A negative-helicity or left-handed (LH) f requires a right-handed (RH) $\bar{f}$ in (2.1). Alternatively, a RH f and a LH $\bar{f}$ must be combined.

The c.m. angular distributions for the two helicity states of a given photon at an angle θ relative to f are shown in Fig. 2, for a LH f and RH $\bar{f}$. For a direct comparison with the scale of the weak-boson cross sections discussed later, the c.m. energies are chosen to be 200 and 600 GeV, although the relative helicity distributions are independent of energy once the fermion mass is neglected. We observe that the photon (either photon) is strongly LH (RH) along the incident f ($\bar{f}$) direction; exactly the opposite configuration dominates for the other choice of RH f and LH $\bar{f}$. Such handedness matching is also seen for hard forward electron bremsstrahlung, studied long ago by McVoy and Dyson.[5,6]

A key ingredient for such results is the fermion-helicity-conserving vector interaction. The importance can be seen by inserting an additional helicity-flipping anomalous-magnetic-moment vertex,

$$\gamma^{\alpha}\rightarrow\gamma^{\alpha}+\frac{1}{4\mu}[\gamma^{\alpha},q]\,, \tag{2.2}$$

where q is the photon four-momentum and μ is some mass scale. Clearly, the nonrenormalizable tensor interaction will dominate the original vector interaction for energies above μ (so the choice of the fermion mass as the scale can lead to ridiculous rates) and we expect to see a change in the previous distributions for such energies. To show the transition, we let $\mu=100$ GeV and we recalculate the angular distributions, keeping LH f and RH $\bar{f}$ for comparison. The results are shown in Fig. 2; indeed, the other photon helicity configuration contributes increasingly with energy. In the limit of energy large compared with μ, we find both helicities with equal probability. [We should also note that, in addition, the tensor interaction of (2.2) permits f and $\bar{f}$ to have the same helicity, where both photon helicity configurations contribute in both forward and backward directions.]

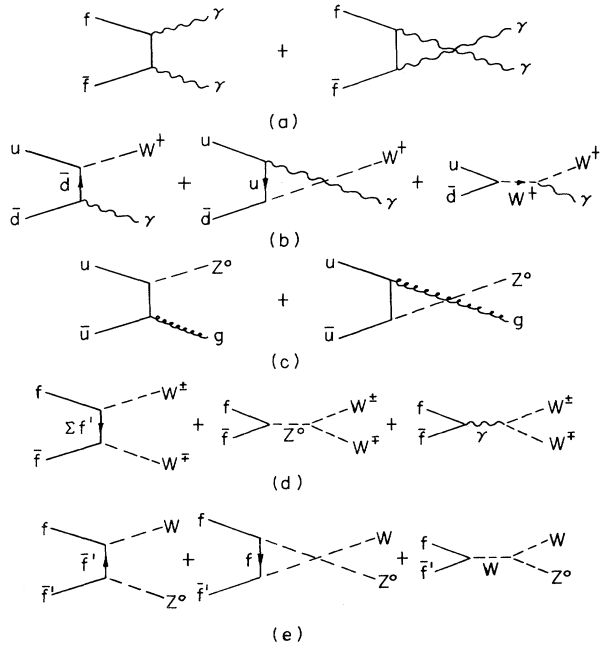

FIG. 1. Feynman graphs for the spin-$\frac{1}{2}$ fermion-antifermion annihilation: (a) $f\bar{f}\rightarrow\gamma\gamma$, (b) $u\bar{d}\rightarrow W\gamma$, (c) $u\bar{u}\rightarrow Zg$, (d) $f\bar{f}\rightarrow WW$, (e) $f\bar{f}'\rightarrow WZ$.

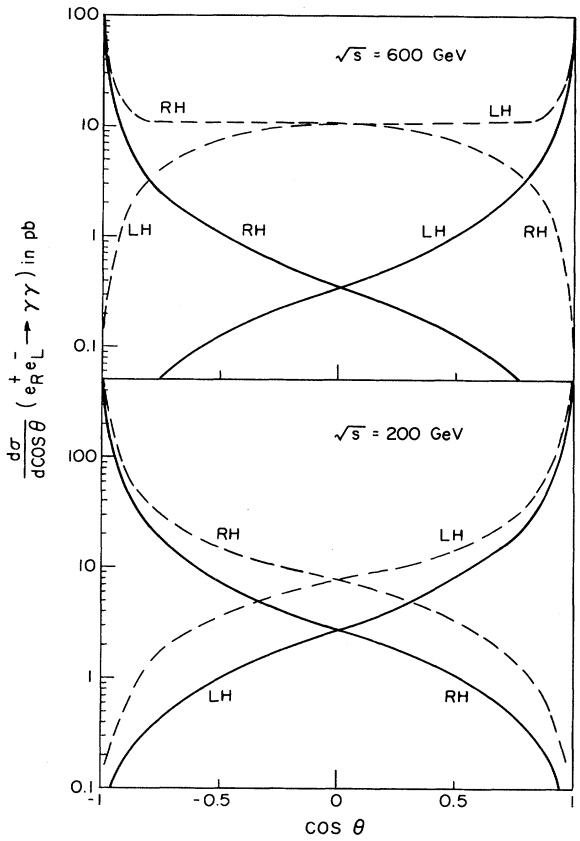

FIG. 2. Photon polarization for $e^+e^-\rightarrow\gamma\gamma$ with RH e^+ and LH e^-. θ is the c.m. angle between a given photon and e^-. The dashed curve is the nonrenormalizable result described in the text. The full θ range gives double the total counts. 1 pb$=10^{-36}$ cm^2.

Another key ingredient in the renormalizable case is the fermion pole which leads to the forward and backward peaking. Were the mass of the internal line not negligible or the interactions not renormalizable, we generally would not see the dominance of the handedness-matching configuration.

The fermion pole explains why angular momentum does not seem to be conserved along the beam direction. The initial state has $J_z=-1$ for the LH fermion moving in the $+z$ direction. But the dominant photon final states, collinear with the beam, correspond to $J_z=-2$ according to Fig. 2. What happens is that as the photon c.m. angle

θ vanishes the Feynman numerators go to zero ($\sim\theta$) due to angular momentum conservation, but the propagator poles diverge faster ($\sim\theta^{-2}$). The collinear divergence represents an infinite amplitude for forward emission by *massless* fermions. An analytical study of $f\bar{f}\to\gamma\gamma$ involving a new technique is given in Sec. VI.

III. W,Z^0 POLARIZATION IN $f\bar{f}'\to W\gamma,Z\gamma,Wg,Zg$

The quark-antiquark annihilation into a weak boson and a photon was proposed several years ago[7] as a channel that could offer a test of the gauge properties of the W. The rate, angular distribution, and (as we shall see) the polarization are very sensitive to the W electromagnetic moments, for example. The Feynman diagrams shown in Fig. 1(b) include a photon coupling to the W. The relatively low threshold means that the $p\bar{p}\to W\gamma X$ experiment lies in the CERN SPS domain;[8] a detailed study including a Monte Carlo analysis of the decay spectra will be presented elsewhere.[9]

A. $f\bar{f}'\to W^{\pm}\gamma$

We first focus on the W polarization[4] in the reaction of Fig. 1(b),

$$u\bar{d}\to W^+\gamma\ , \tag{3.1}$$

in the quark-antiquark c.m. frame. The formulas for the amplitude, the polarization basis, and the polarization density matrix can be found in Refs. 9 and 10.

In general, we use the method of Bjorken and Chen,[11] particularly as practiced by Gaemers and Gounaris.[12] The amplitude for (3.1) has the form

$$A=\bar{v}(k_2)\Gamma(1-\gamma_5)u(k_1) \tag{3.2}$$

with an odd number of γ matrices in Γ. (We neglect the quark masses.) Only LH u and RH $\bar{d}$ contribute, of course. The procedure, which is less cumbersome than the usual calculation, is to multiply and divide A by some other bilinear $\bar{u}\Gamma' v$,

$$A_{LR}=\sum_{\substack{\text{quark}\\ \text{spins}}} A=\frac{\mathrm{Tr}[\not k_2\Gamma(1-\gamma_5)\not k_1\Gamma']}{\bar{u}_L\Gamma' v_R}\ , \tag{3.3}$$

where the freedom to sum over quark spins (inside an unpolarized nucleon) produces a simpler Dirac trace calculation and involves the *amplitude*. The Γ' contains an odd number of γ matrices as well and is chosen to be $\not n$ where $n^{\mu}=(0,\hat{n})$ with $\hat{n}\perp$ the beam.

We present in Fig. 3 differential cross-section results for (3.1) calculated as above for LH, RH, and longitudinally polarized W^+; c.m. energies of 200 and 600 GeV are selected as mentioned for the figures.[13] In Table I the polarization percentages of the total cross section (with cutoffs in the forward and backward directions) is tabulated for each of the three W polarizations. Our numerical work was checked by using rectangular basis for the W polarization states and comparing to curves given by Hellmund and Ranft.[14]

We find that the W^+ is overwhelmingly LH (RH) when it is emitted in the u- ($\bar{d}$-) quark direction. Since these

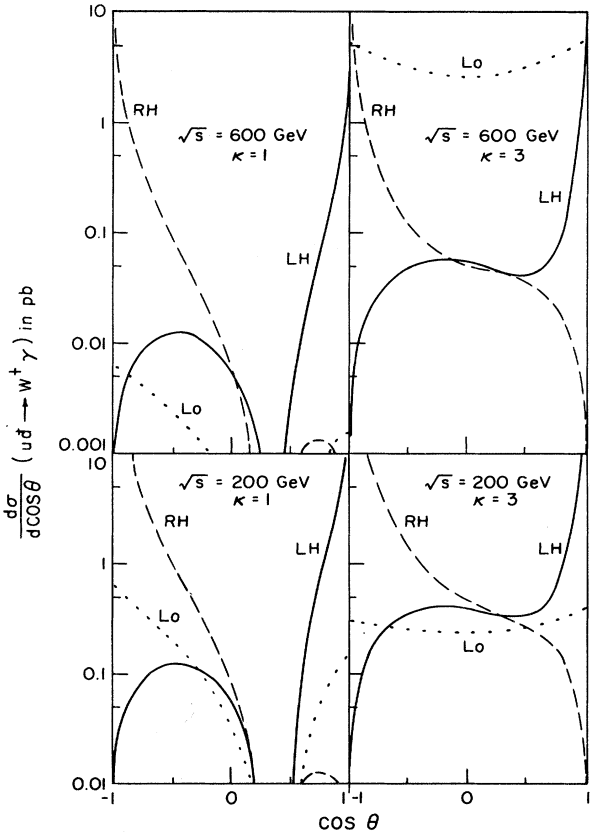

FIG. 3. W^+ polarization for $u\bar{d}\to W^+\gamma$. θ=c.m. angle between W^+ and u. Lo=longitudinal.

configurations are promoted by the fermion propagator poles, we can understand the polarization percentages simply by consideration of the quark electric charges. From the angular distribution and the table about 80% of the events correspond to a (RH) W^+ in the $\bar{d}$ hemisphere (the hemisphere toward which the incident $\bar{d}$ moves) and 20% to a (LH) W^+ in the u hemisphere.[15] Thus the ratio of RH/LH is given very accurately by $(Q_u/Q_{\bar{d}})^2=4$, involving the photon coupling to the quark that is not emitting the W^+. *The forward-backward asymmetry is a measure of the quark charge.* In $\bar{\nu}_e e^-\to W^-\gamma$,[7] the W is mainly in the $\bar{\nu}$ hemisphere in agreement with the neutrino zero charge.

The charge-conjugated reaction $\bar{u}d\to W^-\gamma$ gives the mirror image where about 80% of the W^- are LH and in the d direction. The longitudinal helicity rate is small and rapidly disappears with c.m. energy in both reactions.

If the fermion masses are neglected, the cross sections diverge logarithmically in the forward and backward directions, which is also the case in the $\gamma\gamma$ reaction of Sec. II. These infinities would make it obvious that ratios of the pole residues are all that is required for a determination of the relative cross sections. However, we wish to stress that, even in the presence of cutoffs, an accurate estimate can still be made. The percentages in the tables are insensitive to small cutoffs $\theta_{\min}$ (and $\pi-\theta_{\min}$); the corrections are only of order $\theta_{\min}$.

Another measure of the charges is the familiar

TABLE I. Angular-averaged W^+ c.m. polarization (normalized cross section) for $u\bar{d}\to W^+\gamma$ as a function of c.m. energy. Lo=longitudinal. Even for $\kappa=1$, the relative longitudinal contribution can grow with energy if the forward/backward peaks are suppressed. The end points are cut off by a Gauss-Legendre integration corresponding to $\theta_{\min}=0.4°$, $\theta_{\min}<\theta<\pi-\theta_{\min}$. The weak dependence on $\theta_{\min}$ is noted in the text.

$\sqrt{s}$ (GeV)	κ	% LH	% Lo	% RH
82	1	18.9	3.2	77.9
	2	18.9	3.2	78.0
	3	18.9	3.1	78.0
100	1	18.9	2.9	78.2
	2	19.0	2.5	78.5
	3	19.0	2.4	78.6
200	1	19.3	1.0	79.7
	2	18.8	4.4	76.8
	3	17.1	16.0	66.9
600	1	19.5	0.1	80.4
	2	11.8	40.5	47.7
	3	5.7	72.7	21.6
1000	1	19.5	0.0	80.5
	2	6.7	66.4	26.9
	3	2.4	88.5	9.1

Mikaelian-Samuel-Sahdev zero[16] evidenced in Fig. 3. The position of the zero is $\cos\theta=1+2Q_j$ for $q_i\bar{q}_j\to W^+\gamma$. This is an instance of a general class of spin-independent radiation zeros[17] and is not present for nongauge values, $\kappa\neq1$, in the W g factor, $g=1+\kappa$. The electromagnetic vertex for a charged boson with arbitrary κ can be found in Robinett,[18] for example.

That these reactions follow so closely the pattern of $f\bar{f}\to\gamma\gamma$ is not entirely obvious. With an additional longitudinal polarization state it is now possible to conserve angular momentum along the beam. But in fact that spin state is negligible, according to these results and the calculations in Sec. VI.

For nonrenormalizable photon-W couplings, on the other hand, it is expected that the W longitudinal state will dominate, overwhelming the other spin states at high energy. This is borne out in Fig. 3 and in Table I where $\kappa\neq1$ values are chosen to illustrate such effects.[18] Notice, however, that the RH/LH ratio is still 4.

B. $f\bar{f}'\to Z^0\gamma, Z^0g, W^\pm g$

We turn to the production of Zg, Wg, and $Z\gamma$ (g =gluon) where no trilinear boson coupling is present in the standard model.[19,20] The two (exchange) graphs in

$$u\bar{u}\to Z^0g\ , \tag{3.4}$$

for example, are depicted in Fig. 1(c). The initial/final SU(3) color is to be averaged/summed; otherwise, the calculations proceed as before.

The angular distributions of (3.4) for the three Z^0 polarizations are drawn in Fig. 4, for LH u and RH $\bar{u}$. Since the neutral-current coupling to the u quark is $\frac{1}{3}V-A$ for $\sin^2\theta_W=\frac{1}{4}$, the other choice (RH u, LH $\bar{u}$) contributes at a smaller rate. In either case, we find almost 50% of the events have Z^0 in the u ($\bar{u}$) hemisphere and with its helicity. There is small (3% at 200 GeV) longitudinal contamination at wide angles that decreases with c.m. energy.

The diagrams of Fig. 1(c) and the polarization results are essentially the same for $d\bar{d}\to Z^0g$ (where the d neutral current is $-\frac{2}{3}V+A$ for $\sin^2\theta_W=\frac{1}{4}$); $e^+e^-,q\bar{q}\to Z^0\gamma$; and $q\bar{q}'\to Wg$. The weak boson found in a given fermion hemisphere has the fermion's handedness. The two hemispheres have equal weighting when the gluon (photon) couples symmetrically to either side of the vertex for the emission of a colorless (neutral) boson.

The polarization curves for the photon in $Z^0\gamma$ and the gluon in Z^0g and Wg resemble those in Fig. 2. The polarization curves for the photon in $W\gamma$ resemble the curves

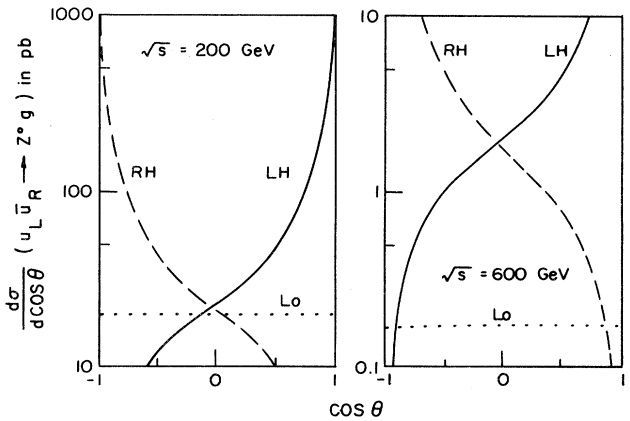

FIG. 4. Z^0 polarization distributions for $u_L\bar{u}_R\to Z^0g$. θ=c.m. angle between Z^0 and u. The gluon coupling corresponds to three generations, $Q^2=s$, and $\Lambda_S=400$ MeV.

TABLE II. Photon polarization as in Table I for $u\bar{d}\to W^+\gamma$.

$\sqrt{s}$ (GeV)	κ	% LH	% RH
82	1	51.5	48.5
	2	51.4	48.6
	3	51.3	48.7
100	1	62.4	37.6
	2	61.9	38.1
	3	61.3	38.7
200	1	78.7	21.3
	2	76.3	23.7
	3	71.7	28.3
300	1	80.0	20.0
	2	75.3	24.7
	3	67.2	32.8

in Fig. 3 (θ is the angle between the photon and the $\bar{d}$) if we reverse the labels, RH↔LH, and ignore the longitudinal curves. The 80% rule is evident here; however, near threshold (see Table II), or for nonrenormalizable couplings at high energy, both photon helicities are equally probable at all angles.

IV. W,Z^0 POLARIZATION IN $f\bar{f}'\to WW,WZ,ZZ$

The other trilinear self-coupling in the GWS model is the WWZ vertex and contributes to the production of WW and WZ pairs in fermion-antifermion annihilation. The reaction,

$$f\bar{f}\to W^+W^- \tag{4.1}$$

is diagrammed in Fig. 1(d) and involves both WWZ and $WW\gamma$ couplings. The reaction in Fig. 1(e)

$$f\bar{f}'\to W^{\pm}Z^0\,, \tag{4.2}$$

has no photon coupling. Rounding out this system is

$$f\bar{f}\to Z^0Z^0\,, \tag{4.3}$$

where boson self-couplings would only arise in unorthodox models; the diagrams are structured like Fig. 1(a).

The CERN LEP reaction, $ee\to WW$, has received the earliest (and most) attention[21] in plans to establish experimentally the existence of the WWZ gauge self-coupling. Perhaps this may also provide an accurate measurement of M_W, depending on the degree to which the threshold is smeared by width effects. The reaction $ee\to Z^0Z^0$ has also been suggested[22] where anomalous Z^0 couplings[12] could be probed.

Another test of the WWZ vertex has been proposed[7,22] using Drell-Yan annihilation into WW and WZ^0. [$f=q$, $f'=q'$ in (4.1)–(4.3); Z^0Z^0 is likewise present at roughly the same cross-section level.[22]] This may be measurable in future facilities such as the Fermilab Tevatron.[23]

We have calculated the polarization for both e^+e^- and $q\bar{q}'$ annihilation into such weak-boson pairs.[4] (Only WZ^0 cannot be formed from e^+e^-.) The amplitude method described in the previous section is also employed here. To show most clearly the predominant helicity at a given angle in the electron or quark c.m. reference frame, we again plot differential cross sections for the various helicities of the $W^{\pm}$ and Z^0. The programs used in this work were spot checked against the differential cross sections given in terms of a rectangular polarization basis (where the helicity phase or handedness is unavailable) for[12] e^+e^- and[14] $q\bar{q}'$.

A. $f\bar{f}\to W^{\pm}W^-$

The results for $ee\to WW$ at the energies chosen for comparison with $q\bar{q}$ are shown in Fig. 5. Included in the figure are the corresponding curves for a nongauge (nonrenormalizable) value of the W magnetic moment parameter κ.

The handedness rule is observed. With only $V-A$ lepton interactions and only the t-channel pole (neutrino propagator) enhancement—there is no crossed u-channel pole—the W^+ (W^-) lies predominantly in the e^+ (e^-) hemisphere and is predominantly RH (LH) in that hemisphere, even for the lower energy. On the other hand, the longitudinal polarization dominates the other spin states at 600 GeV for the nongauge $\kappa=3$ value, except for the very-small-forward-angle region. The averaged polarizations shown in Table III for several energies and κ values reflect this striking contrast, except near threshold where the three helicities are more or less equally represented for all κ values. (At threshold, all invariants $\sim M_W{}^2$ and the

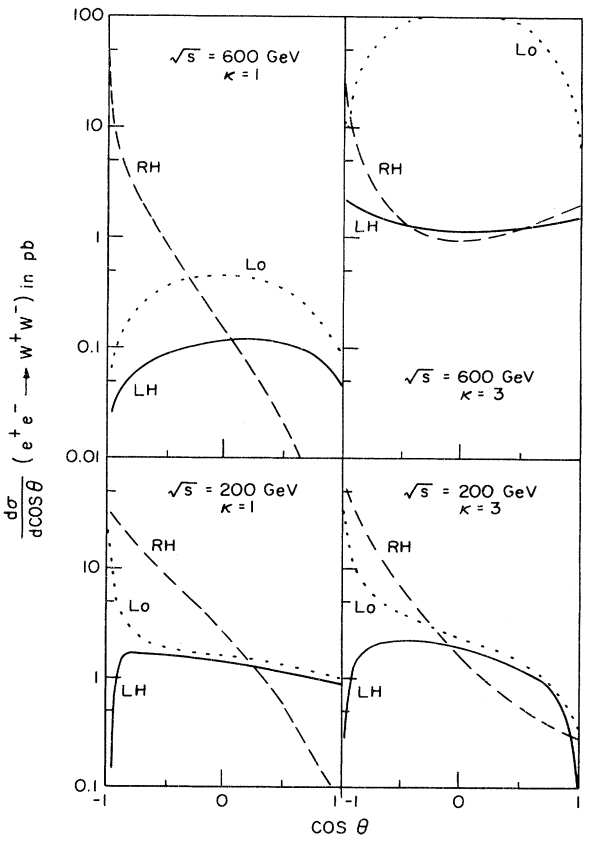

FIG. 5. W^+ polarization for $e^+e^-\to W^+W^-$. θ=c.m. angle between W^+ and e^-.

TABLE III. W^+ polarization as in Table I but for $e^+e^- \to W^+W^-$.

$\sqrt{s}$ (GeV)	κ	% LH	% Lo	% RH
162	1	28.4	32.7	38.9
	2	28.4	32.6	39.0
	3	28.3	32.8	38.9
180	1	19.4	27.5	53.0
	2	19.7	26.8	53.5
	3	19.2	30.1	50.7
200	1	15.1	22.9	62.0
	2	15.3	22.4	62.2
	3	14.6	31.7	53.7
600	1	3.2	11.0	85.8
	2	1.7	85.0	13.3
	3	1.6	93.9	4.4

t-channel pole is far from the physical region.)

The situation is similar for quark annihilation.[24] The counterpart curves for $u\bar{u} \to WW$ are given in Fig. 6. The difference compared with e^+e^- in the sign of the fermion charge pushes the LH W^+ (RH W^-) into the u ($\bar{u}$) hemisphere. The $d\bar{d} \to WW$ curves in Fig. 7 reverse the helicities once again.

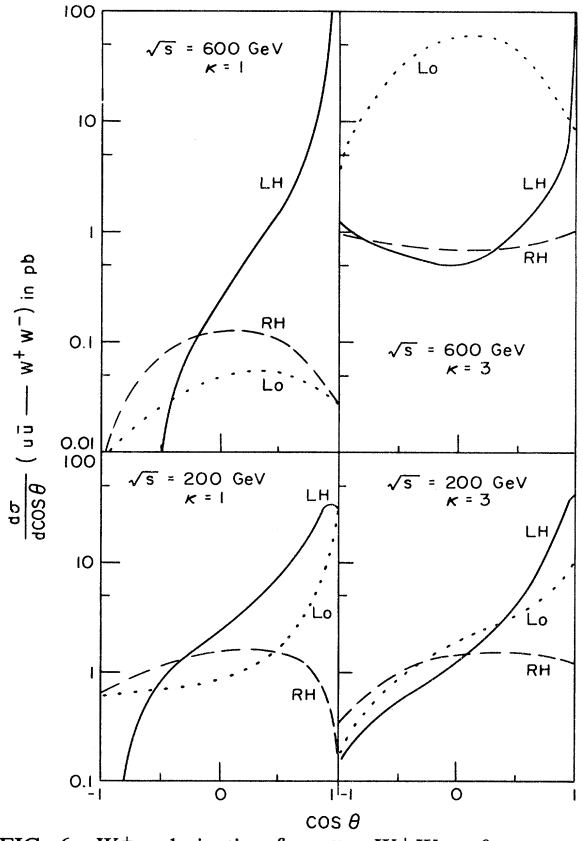

FIG. 6. W^+ polarization for $u\bar{u} \to W^+W^-$. θ=c.m. angle between W^+ and u.

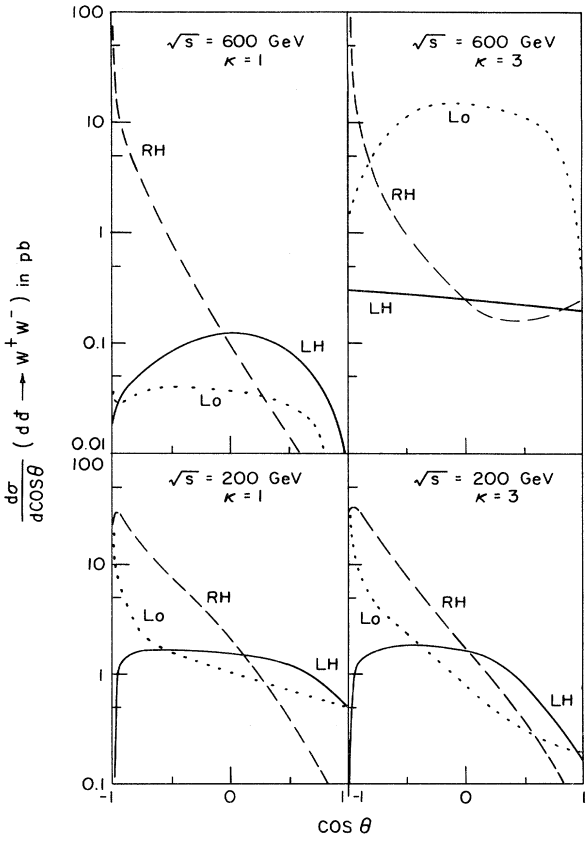

FIG. 7. W^+ polarization for $d\bar{d} \to W^+W^-$. θ=c.m. angle between W^+ and d.

In spite of the large W mass, the neutrino propagator pole is close to the physical forward scattering region for the energies considered. An expansion of the propagator denominator reveals delicate cancellations of the two leading terms in W energy. Therefore the suppression expected from angular momentum conservation along the beam directions, like that discussed for $f\bar{f} \to \gamma\gamma$ in Sec. II, is offset by the pole. Still, a zero along the beam is expected for the production of a RH W recoiling against a LH W, for example, although the cosθ scale in Figs. 5—7 is too coarse in most cases to show this.

There are other ways of introducing nongauge values into WW production, while still consistent with presently known experimental constraints. One modification is to consider $\kappa_Z \neq 1$ where κ_Z is the analogous "magnetic moment" parameter[18] for the coupling of Z^0 to the $W^\pm$. The changes encountered as we shift κ_Z resemble the changes gotten from shifting κ. Table IV displays the average polarization for $d\bar{d} \to WW$ for different κ_Z.

B. $f\bar{f}' \to W^\pm Z^0$

The general annihilation channel $f\bar{f}' \to WZ$ also requires LH fermions and RH antifermions. Hence the boson we find in the f ($\bar{f}'$) hemisphere will be LH (RH) according to the handedness rule. (Both poles are present so that each hemisphere gets the necessary enhancement, after the gauge coupling cancellations.) This is verified in

TABLE IV. W^+ polarization as in Table I but for $d\bar{d}\to W^+W^-$. κ_z is the weak-magnetic-moment parameter for the WWZ coupling. $\kappa=1$.

$\sqrt{s}$ (GeV)	κ_z	% LH	% Lo	% RH
200	1	14.6	20.2	65.2
	2	14.3	33.8	51.9
	3	12.6	54.5	32.8
600	1	3.2	1.7	95.2
	2	1.7	92.0	6.3
	3	1.6	95.6	2.7
1000	1	2.3	0.8	96.9
	2	0.6	98.0	1.4
	3	0.6	98.6	0.8

Figs. 8 and 9, where the angular polarization of the W^+ and of the Z^0 for $u\bar{d}\to W^+Z^0$ is illustrated.

The relative population of each hemisphere (and hence of each circular polarization) is also found simply. The ratio of the cross section for Z^0 emitted into the f hemisphere to the cross section for Z^0 emitted into the $\bar{f}'$ hemisphere is simply $(g_V-g_A)^2/(g'_V-g'_A)^2$ which is $(\frac{4}{5})^2$ for $u\bar{d}$ and $\sin^2\theta_W=\frac{1}{4}$. This is verified for the average

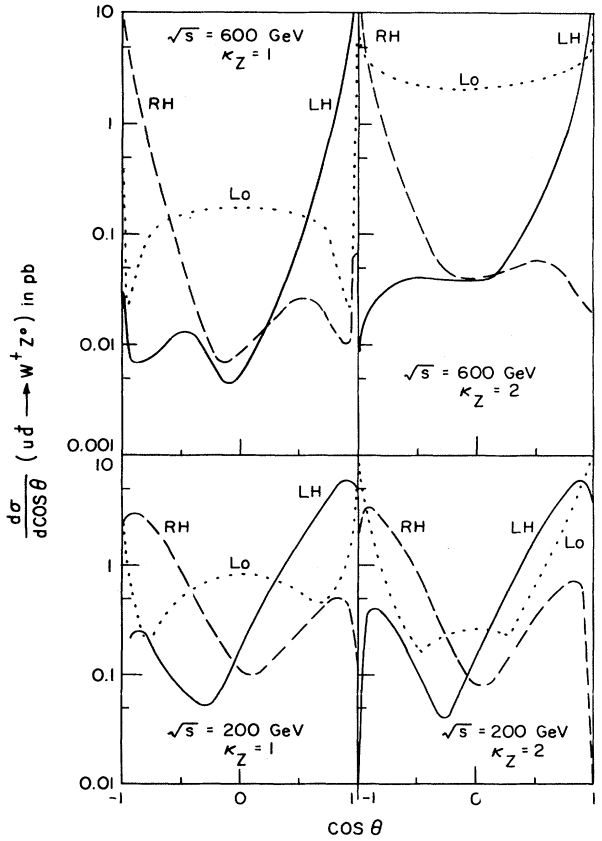

FIG. 8. W^+ polarization for $u\bar{d}\to W^+Z^0$. θ=c.m. angle between W^+ and u.

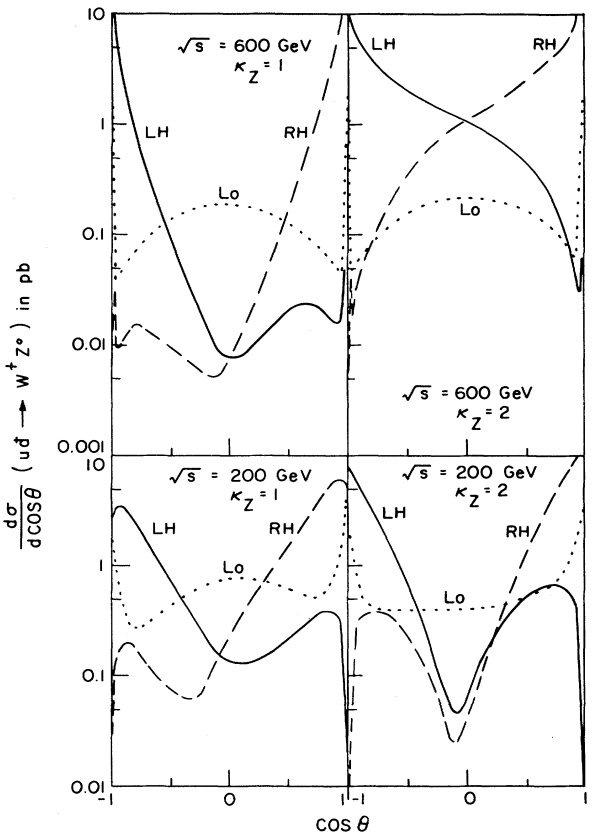

FIG. 9. Z^0 polarization for $u\bar{d}\to W^+Z^0$. θ=c.m. angle between Z^0 and $\bar{d}$.

polarization seen in Table V (calculated for $\sin^2\theta_W=0.23$). Accordingly, the W^+ polarization probabilities are reversed (Table VI).

In Fig. 9 and Table V, as in Fig. 4, the longitudinal polarization is under control since the Z^0 is coupled to a conserved current in the high-energy limit even for $\kappa_Z\neq 1$. For $\kappa_Z\neq 1$, however, the LH and RH results grow with energy, failing to satisfy the handedness rule and its associated ratio: The longitudinal W is *not* under control (Fig. 8).

Again it should be mentioned that certain zeros expected from angular momentum conservation at $\theta=0,\pi$ are not shown in Figs. 8 and 9. For example, the RH W^+

TABLE V. Z^0 polarization as in Table I but for $u\bar{d}\to W^+Z^0$. κ is irrelevant.

$\sqrt{s}$ (GeV)	κ_z	% LH	% Lo	% RH
200	1	27.6	25.8	46.6
	2	31.8	20.0	48.2
	3	38.5	13.3	48.3
400	1	36.1	8.4	55.5
	2	43.2	2.8	53.9
	3	47.4	1.3	51.3
600	1	37.0	6.6	56.4
	2	45.7	1.1	53.3
	3	48.7	0.3	51.0

TABLE VI. W^+ polarization for $u\bar{d}\to W^+Z^0$ as in Table I. κ is irrelevant.

$\sqrt{s}$ (GeV)	κ_z	% LH	% Lo	% RH
200	1	45.4	27.0	27.5
	2	40.8	33.6	25.6
	3	27.4	54.2	18.4
400	1	55.2	8.9	35.9
	2	33.7	43.9	22.3
	3	14.4	75.6	10.0
600	1	56.2	6.8	36.9
	2	24.4	59.4	16.2
	3	8.7	85.2	6.0

curve actually returns to zero at $\theta=0$ in Fig. 8. There is much intricate structure in the forward and backward directions due to the combination of helicity constraints, approximate current conservation, and pole enhancements.

C. $f\bar{f}'\to Z^0Z^0$

The last annihilation channel (4.3) most closely parallels the $\gamma\gamma$ channel of Sec. II. The longitudinal polarization is increasingly negligible with higher energy; each Z^0 is coupled to a conserved current in this reaction. Since $\sin^2\theta_W\cong\frac{1}{4}$, no fermion helicity is projected out. Therefore we require information on the initial spin states to apply the rule which says that the Z^0 has the same handedness as the fermion in whose hemisphere it lives. Figure 10 shows the 50% occupancy rate for RH e^+ and LH e^- in $ee\to ZZ$.

V. POLARIZATION FOR SINGLY PRODUCED W,Z^0

The handedness rule also applies rather nicely to those single-boson production reactions where the $W^\pm$ and Z^0 have been emitted by fermions. The parent fermion polarization is again seen to be the determining factor.

A. $e^+e^-\to Z^0; p\bar{p}(pp)\to W^\pm, Z^0+X$

These much studied reactions are included, not just for completeness, but also to consider another application of the rule. Handedness matching can be seen to apply in reference frames obtained by a Lorentz boost into either fermion hemisphere from the annihilation $f\bar{f}'$ rest frame.

The vector–axial-vector coupling in $ee\to Z^0$, which is mainly axial-vector for $\sin^2\theta_W\cong\frac{1}{4}$, requires that the Z^0 have ±1 spin projection along the c.m. beam direction. (The longitudinal state is not produced in the limit of zero electron mass.) Therefore the LH e^-–RH e^+ combination leads to a LH(RH) Z^0 when the Z^0 is boosted in the e^- (e^+) direction. In any frame where the Z^0 is moving parallel to a given lepton's initial direction, the Z^0 handedness matches that of the lepton.

The boosts have more relevance in proton colliders since $q\bar{q}'$ annihilation generally involves a moving c.m. frame. As above, noting only that W production fixes the quark helicities, a W^+ produced in motion along the u quark ($\bar{d}$ antiquark) is LH (RH). Similarly the W^- is emitted by the $\bar{u}$ (d) into a RH (LH) state.

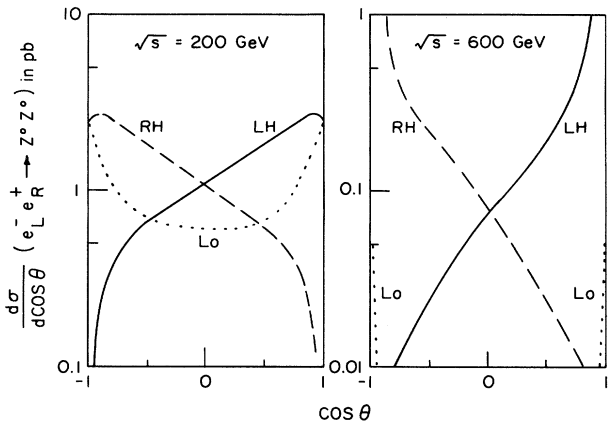

FIG. 10. Z^0 polarization for $e_L^-e_R^+\to Z^0Z^0$. θ=c.m. angle between a given Z^0 and e^-.

Given this description, the W helicity analysis leads to a well-known $e^\pm$ decay asymmetry[25] that will provide a test of the W hypothesis for the recent $p\bar{p}$ event. The RH e^+ (LH e^-) always favors the $\bar{d}$ (d) direction. The decay lepton (antilepton) follows the proton (antiproton) direction. With a W intermediate state, we may say the lepton follows the quark helicity and direction and the antilepton follows the antiquark helicity and direction.

Production of Z^0 by $u\bar{u}$ or $d\bar{d}$ annihilation involves neutral currents for which both LH and RH interactions are allowed. (There is no pronounced asymmetry in the Z^0 decay.) The situation is similar to $e^+e^-\to Z^0$; the LH q–RH $\bar{q}$ combination leads to a LH Z^0 in the proton direction, and vice versa.

B. Single production with recoil

The early searches for W's centered on neutrino disintegration into the weak boson during an electromagnetic recoil off a nuclear target,[26]

$$\nu_l+N\to W+l+X\ . \tag{5.1}$$

The polarization of the W produced in this way has been studied in some detail.[27,28]

The result found is that the W follows predominantly the handedness of the neutrino. The important contribution comes from the electromagnetic recoil of the (light) final charged lepton; the lepton propagator pole is the deciding factor controlling the W polarization.[27] (There is an important cancellation between the two graphs corresponding to the recoil of l and W, respectively.) In Fig. 11(a) the electroweak four-body subgraphs of (5.1) are drawn in a suggestive fashion. The presence of a diagram with a t-channel pole enhancement implies that we should indeed see a LH W^+ (RH W^-) emitted along the ν_l ($\bar{\nu}_l$).

There are differences in the present application. Since we are not in the $\nu\gamma$ c.m. frame, a Lorentz transformation is required to connect the two reference frames. Also, renormalizability is not critical; the u-channel diagram in

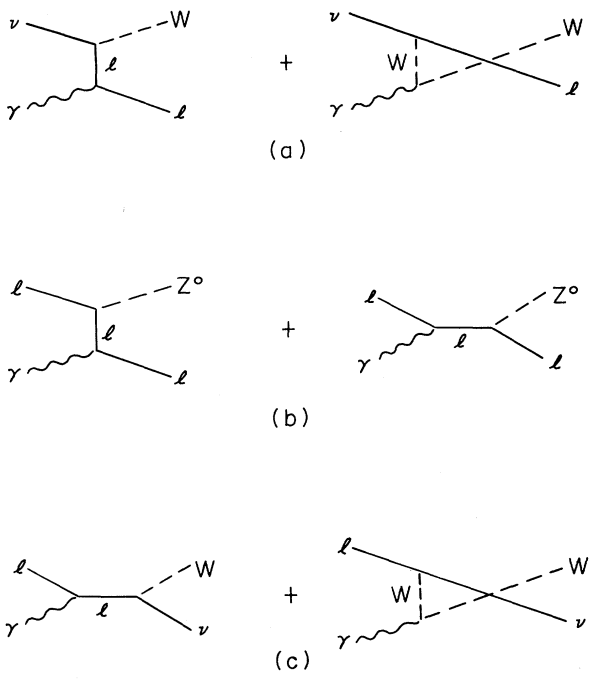

FIG. 11. Feynman graphs for the lepton—(virtual-)photon Compton-type reactions: (a) $\gamma\nu_l \to Wl$, (b) $\gamma l \to Zl$, (c) $\gamma l \to W\nu_l$.

Fig. 11(a) is less important[28] for $\kappa \neq 1$ than for $\kappa = 1$. As in bremsstrahlung[7] the two-body c.m. energy is minimized. Unlike bremsstrahlung, the t-channel diagram is dominant for nonzero M_W, yet the handedness rule accurately describes both reactions.

The same description applies to Z^0 production,[29,30]

$$l + N \to Z^0 + l + X \ , \tag{5.2}$$

where the lepton propagator is likewise dominant. The diagrams analogous to Fig. 11(a) are shown in Fig. 11(b). The handedness depends on the initial lepton helicity, recalling that the charged-lepton—Z^0 coupling is essentially axial vector in character.

The handedness rule is seen to be consistent with another reaction where the W polarization is *not* dominated in general by an initial lepton. The line-reversal of (5.1) is[31]

$$l + N \to W + \nu_l + X \ , \tag{5.3}$$

with the subgraphs illustrated in Fig. 11(c). There is no lepton-exchange pole in this case and, indeed, the calculations[31,32] show no dominant handedness. The W polarization is sensitive to its photon coupling and does not follow the initial l polarization in so simple a manner.

We should remark about the relevance of (5.2) and (5.3). Both reactions are in the energy regime of proposed ep colliders.[33] However, the theoretical rates are too low to be of primary interest. Another version of (5.3),

$$e^+ + e^- \to W + \nu + e \ , \tag{5.4}$$

also has a cross section that is rather small.[34]

VI. HELICITY ANALYSIS

It is possible to give an economical analytic demonstration of the correlation between a fermion parent and an emitted photon through the use of the elegant polarization basis developed recently by the CALKUL group.[35] In this way we can build a connection between well-known QED processes such as photon pair production, with which we introduced our study in Sec. II, and, by a generalization of the CALKUL basis to massive weak bosons, the new territory of electroweak boson production.

Choose the momentum and polarization assignments for the e^+e^- version of (2.1) to be

$$e_L^-(k_1) + e_R^+(k_2) \to \gamma(p_1,\epsilon_1) + \gamma(p_2,\epsilon_2) \ .$$

Ignoring overall constants, the amplitude is

$$M(e_L^- e_R^+ \to \gamma\gamma) = \bar{v}(k_2) T (1-\gamma_5) u(k_1) \ , \tag{6.1a}$$

with

$$T(\epsilon_1,\epsilon_2) = \not{\epsilon}_2(\not{p}_1 - \not{k}_1)^{-1}\not{\epsilon}_1 + \not{\epsilon}_1(\not{k}_2 - \not{p}_1)^{-1}\not{\epsilon}_2 \ . \tag{6.1b}$$

Outgoing polarization vectors are understood in (6.1a) and the $e^{\pm}$ are taken to be massless.

The basis

$$\epsilon^{\pm} = \frac{1}{\sqrt{2}}(\epsilon^{\parallel} \pm i\epsilon^{\perp}) \ , \tag{6.2}$$

corresponding to an *outgoing* RH(+) or LH (−) photon can be used for ϵ_1 with the covariants,[36]

$$\epsilon_\mu^{\parallel}(p_1) = \frac{N}{\sqrt{2}}(k_1\cdot p_1 k_{2_\mu} - k_2\cdot p_1 k_{1_\mu}) \ , \tag{6.3a}$$

$$\epsilon_\mu^{\perp}(p_1) = \frac{N}{\sqrt{2}}\epsilon_{\mu\alpha\beta\gamma}k_1^\alpha k_2^\beta p_1^\gamma \ , \tag{6.3b}$$

where

$$N = (k_1\cdot k_2 k_1\cdot p_1 k_2\cdot p_1)^{-1/2} \ . \tag{6.4}$$

The identity that is particularly effective for (6.1a) is

$$\not{\epsilon}^{\pm}(p_1) = \frac{N}{4}[\not{k}_2\not{k}_1\not{p}_1(1\mp\gamma_5) - \not{p}_1\not{k}_2\not{k}_1(1\pm\gamma_5) \pm 2k_1\cdot k_2\not{p}_1\gamma_5] \ , \tag{6.5}$$

derivable from (6.2) and (6.3).

With terms disappearing by chirality mismatch and by massless Dirac projection [note that the axial-vector current is also conserved; the $\not{p}_1\gamma_5$ term in (6.5) is thereby eliminated], and with propagator denominator cancellation, (6.1) and (6.5) combine to give

$$T(\epsilon^+,\epsilon_2) + N(k_2\cdot p_2\not{\epsilon}_2 + k_2\cdot\epsilon_2\not{p}_1) \ , \tag{6.6a}$$

$$T(\epsilon^-,\epsilon_2) = N(k_1\cdot p_2\not{\epsilon}_2 + k_1\cdot\epsilon_2\not{p}_1) \ . \tag{6.6b}$$

The sandwiching of T in (6.1a) is always understood. For example, we may replace $\not{p}_1$ by $-\not{p}_2$ in (6.6).

When photon 1 is along the electron ($p_1 \to k_1, p_2 \to k_2$) the pole in N is canceled in (6.6a) but not in (6.6b). [One can see that $N \sim \theta^{-1}$ but that its coefficient $\sim\theta^2$ in (6.6a) for a small c.m. angle between p_1 and k_1. On the other

hand, the coefficient in (6.6b) does not vanish as $\theta\to 0$.] The reverse is true for photon 1 along the positron. The handedness matching from $e^{\pm}$, shown in Fig. 2, is thusly verified.

While the details will not be given, we have rederived (using the CALKUL basis) the bremsstrahlung matrix elements and hence the results obtained by McVoy and Dyson.[5,6] [One must recognize in such a derivation that overall phases may differ, so that $a+ib$ is equivalent to $(a^2+b^2)^{1/2}$, for example.] With our technique it appears that one Feynman diagram (s-channel pole) is responsible for the handedness matching when the photon is hard, and the other diagram (exchange) corresponds to the opposite handedness for the photon, when the photon is soft. This is misleading because the use of (6.5) mixes the two contributions; N has the singularities of *both* diagrams.

A radiation representation[37] for

$$u(k_1)+\bar{d}(k_2)\to\gamma(p_1,\epsilon)+W^+(p_2,\eta)\ ,$$

which implements the full radiation symmetry (exhibiting the radiation zero), nicely simplifies the next amplitude of interest. We have

$$M(u\bar{d}\to\gamma W)=Z\bar{v}(k_2)T(1-\gamma_5)u(k_1)\ , \tag{6.7a}$$

ignoring constants. As in (6.1),

$$T(\epsilon,\eta)=\not\eta(\not p_1-\not k_1)^{-1}\not\epsilon+\not\epsilon(\not k_2-\not p_1)^{-1}\not\eta\ . \tag{6.7b}$$

The zero resides in

$$Z=(\tfrac{1}{3}k_1\cdot p_1-\tfrac{2}{3}k_2\cdot p_1)/p_1\cdot p_2\ . \tag{6.7c}$$

Although $p_2{}^2=M_W{}^2\neq 0$, we have a QED-like form where *both* bosons are coupled to conserved fermion currents. This is precisely where the CALKUL basis is so effective.[38] We obtain (6.6) again, replacing ϵ_2 by η.

The photon handedness (Table II) immediately follows, for high energies where M_W is neglected, from (6.6) and (6.7a), including the ratio $[Z(\theta=0)/Z(\theta=\pi)]^2=4$. Near threshold, where $E_\gamma\ll M_W$, we compute that both $T(\epsilon^{\pm},\eta)\cong NM_W{}^2/\sqrt{2}$. The soft photon is emitted unpolarized from either pole, in agreement with Table II.

To study the W polarization in $u\bar{d}\to W\gamma$, we generalize the covariant polarization basis to a *massive* vector boson.[39] In terms of (6.3),

$$\eta_{\pm}=\frac{1}{\sqrt{2}}(\eta^{\parallel}\pm i\eta^{\perp})\ , \tag{6.8}$$

with

$$\eta_\mu^{\perp}(p_2)=-\epsilon_\mu^{\perp}(p_1)\ , \tag{6.9a}$$

$$\eta_\mu^{\parallel}(p_2)=\epsilon_\mu^{\parallel}(p_1)-\frac{p_2\cdot\epsilon^{\parallel}(p_1)}{p_2\cdot p_1}p_{1\mu}\ . \tag{6.9b}$$

The longitudinal basis vector is chosen to be

$$\eta_\mu^{\mathrm{Lo}}=\frac{1}{M_W p_2\cdot p_1}(p_2\cdot p_1 p_{2_\mu}-M_W{}^2 p_{1_\mu})\ , \tag{6.10}$$

which is properly directed along $\vec{p}_2$ in the c.m. frame. It is seen that the triplet $(\vec{\eta}^{\perp},\vec{\eta}^{\parallel},\vec{\eta}^{\mathrm{Lo}})$ gives the correct right-handed basis upon a boost to the W rest frame. (Choose $\vec{p}_1$ antiparallel to the spin quantization axis $\hat{z}$.) In terms of (6.5),

$$\not\eta^{\pm}=\not\epsilon^{\mp}(p_1)-\frac{1}{\sqrt{2}}\frac{p_2\cdot\epsilon^{\parallel}(p_1)}{p_2\cdot p_1}\not p_1\ . \tag{6.11}$$

We build on the photon helicity amplitudes $T(\epsilon^{\pm},\eta)$ already found in (6.6) and insert (6.9)—(6.11) as the case warrants. Detailed calculations yield

$$T(\epsilon,\eta)=\frac{k_1\cdot k_2}{p_1\cdot p_2}\not p_1 R(\epsilon,\eta)\ , \tag{6.12}$$

where

$$R(\epsilon^{\pm},\eta^{+})=\frac{-1}{k_1\cdot p_1}\times\begin{cases}M_W{}^2/(2k_1\cdot k_2)\\ 1\end{cases}\ , \tag{6.13a}$$

$$R(\epsilon^{\pm},\eta^{-})=\frac{1}{k_2\cdot p_1}\times\begin{cases}1\\ M_W{}^2/(2k_1\cdot k_2)\end{cases}\ , \tag{6.13b}$$

$$R(\epsilon^{\pm},\eta^{\mathrm{Lo}})=-NM_W\ . \tag{6.13c}$$

These results apply to and agree with the renormalizable results in Fig. 3 (and 4) and Table I (and II). Even down to threshold (where we go smoothly into the resonance helicity rules discussed in Sec. V A), there is W handedness matching from both u and $\bar{d}$. A pole is reached for the W in the u ($\bar{d}$) hemisphere only for η^- (η^+); there is no pole from η^{Lo}. (In the collinear regions: $p_1'\to\theta$, $k_i\cdot p_1\to\theta^2$, $N\to\theta^{-1}$.) We see again that both photon polarizations contribute equally near threshold.

A covariant basis can be similarly constructed and applied in the WW and WZ channels, for an analysis corresponding to Figs. 5—10 and Tables III—VI. (Now W and Z are not coupled to conserved currents; threshold polarization is mixed.) We may also use such a basis to see rather directly the handedness, or lack of handedness, in the single W production of Sec. V B. In contrast to electron bremsstrahlung, the spin terms in the exchange graph for $\nu N\to lWX$, for example, lead to handedness matching, essentially a finite-M_W effect. Finally we mention that it is easy to do numerical work with such helicity amplitudes.[39]

VII. CONCLUSIONS

The principal objective has been to provide polarization information, as a function of energy and angle, that may be helpful in estimating decay spectra[8] in various W production experiments. The particular relevance of the polarization lies in the tendency of the RH $\bar{f}$ to follow, and the LH f to move opposite to, the W spin in the rest-frame decay $W\to f\bar{f}$. This leads[25] to a "hole" in the e^+ (e^-) event rate, for instance, along the proton (antiproton) in single-W production (Sec. V A).

Asymptotically, a forward-emitted W follows the handedness of its parent, so that the dominant contributions, at high energy, to $p\bar{p}\to WW$ and WZ have exactly the same suppression (holes) in the $e^{\pm}$ rates along the beams. ($W\gamma$ has the same holes at all energies.) But the $q\bar{q}'\to WW, WZ$ cross sections are larger near threshold where all polarization states are present. This gives prom-

ise to the possibility that a window may occur for the detection of WW and WZ pairs, in spite of the single-W background (ironical as that sounds).

The calculations have been performed in the quark or lepton c.m. frame. This remains convenient for those Monte Carlo programs that can integrate in any frame. Also, the definite handedness means that the lepton/quark decay spectrum in the W rest frame is $(1\pm\cos\psi)^2$, where ψ is defined relative to the c.m. direction of the W. This angular distribution is easily boosted to the frame of interest.

We have further strived to unify the description of the spin and angular distributions for gauge bosons produced in various collisions. While the focus has been on boson pair production, due to quark or electron annihilation, the larger picture of hard-boson bremsstrahlung by any parent quark or lepton should be kept in mind. We have defined the parent *hemisphere* to be the forward (2π solid angle) hemisphere into which the parent is moving, with the equatorial plane perpendicular to its initial motion. We have in addition introduced the phrase "handedness matching" to describe that situation where the emitted boson has the same handedness as the parent fermion, either right-handed or left-handed, but not longitudinal.

The first general conclusion of the calculations is that the relevant diagrams for the bremsstrahlung of weak bosons (or other gauge bosons) exhibit handedness matching just as in QED. This is not so obvious because an appreciable longitudinal state might be expected to survive to a greater degree than it does, particularly since, in contrast to QED, angular momentum can now be conserved in pair production in the forward direction.

The second general conclusion is that, for renormalizable gauge theories, the presence of boson-emission graphs whose propagator poles lie on the edge of phase space (forward or backward divergences) dominate emission into the associated hemisphere.

Hence we find a rule from the two conclusions. We say that there is dominance of handedness matching over the hemisphere from the appropriate parent in the presence of a pole at the collinear configuration. There may be an analogous effect from the other parent. Also, two or more diagrams with the same pole position would interfere accordingly. In general, such poles dominate the event rate and the polarization.

Of course the parents' polarization is fixed by the W coupling. The Z^0 coupling, on the other hand, is increasingly axial-vector in the sequence $\nu\to d\to\bar{u}\to e^-$.

The handedness rule is quantitatively very useful, as observed in the numerical presentation, since the hemispherical event rate is generally proportional to the (square of the) couplings, even with sizable cuts taken to exclude the pole(s). For example, $W\gamma$ production is well described, both in the number of events and in the degree of polarization, by merely comparing the parents' electric charges. This suggests a way to measure these charges and to check the source of the photon emission. The formula may be written

$$P_i=\frac{g_i^{\,2}}{\sum g_j^{\,2}}\ , \tag{7.1}$$

where P_i is the event or spin (or other?) probability in terms of the residues (couplings g_i). In $u\bar{d}\to W\gamma$, for instance,[40]

$$P(\gamma \text{ spinning off } u)=Q_u^{\,2}/(Q_u^{\,2}+Q_{\bar{d}}^{\,2})=\tfrac{4}{5}\ . \tag{7.2}$$

The accuracy of such formulas, well within a few percent at the higher energies studied in this paper, is in certain cases just as good at the lower energies. The relevant scale, seen from the tables and figures, is the weak-boson mass, except in the channels where one boson is the photon or gluon. Accordingly handedness matching holds down to threshold for the W,Z but not for the soft photon/gluon. The rest-frame helicity argument of Sec. V applies only to the W,Z.

The helicity picture is generally changed for nonrenormalizable (nongauge) couplings at higher energies. In the production of massive vector bosons, this is caused by the (familiar) dominance of longitudinal polarization. We also saw how a tensor interaction mixed both helicities in both hemispheres for $ee\to\gamma\gamma$. Thus the fact that we can specify a unique polarization in a given hemisphere is a direct consequence of good high-energy behavior: *The handedness rule is related to renormalizability.*

The parallel with QED, where we have both fermion helicity conservation and fermion-boson handedness matching, is clearly the lesson of our study. The conservation of helicity for W scattering from an arbitrary electromagnetic field, which holds for gauge couplings,[41] and the handedness transfer are generalizations of the helicity effects in the scattering of photons and electrons and quarks (and of gluons and quarks). Details of collinear divergences, which are sometimes suppressed by the spinor numerators (helicity constraints) in electroweak pair production, resemble the forerunner, $ee\to\gamma\gamma$. The covariant photon polarization basis[35] has also been generalized in the helicity-amplitude analysis discussed in Sec. VI.

ACKNOWLEDGMENTS

The authors are grateful to David Cline for discussions, for his interest, and for detailing the importance of W polarization in the detection of W decay. We are also grateful to Charles Goebel for steering us to the helicity-matching notion in QED. We wish to thank Maurice Jacob for the hospitality of the theory group at CERN where the writing of this article was completed, Larry Trueman for discussions concerning helicity conservation in collinear configurations, and Kenneth Kowalski for a careful reading of the manuscript. We have been supported by the National Science Foundation; C.L.B. is a T.K. Glennan Foundation Fellow.

[1]G. Arnison *et al.*, Phys. Lett. 122B, 103 (1983); 126B, 398 (1983); M. Banner *et al.*, *ibid.* 122B, 476 (1983).

[2]M. Veltman, Phys. Lett. 91B, 95 (1980); W. J. Marciano and A. Sirlin, Phys. Rev. Lett. 46, 163 (1981); C. H. Llewellyn Smith and J. A. Wheater, Phys. Lett. 105B, 486 (1981).

[3]A review is given by F. E. Paige, in Topical Conference on the Production of Particles in Super High Energy Collisions, Madison, Wisconsin, 1979 [Brookhaven Report No. BNL-27066, 1979 (unpublished)].

[4]Some of our results have been reported previously by R. W. Brown, in *Proton-Antiproton Collider Physics—1981,* edited by V. Barger, D. Cline, and F. Halzen (AIP, New York, 1982), p. 251; by C. L. Bilchak, R. W. Brown, and J. D. Stroughair, Bull. Am. Phys. Soc. 27, 675 (1982); and by C. L. Bilchak and R. W. Brown, *ibid.* 28, 752 (1983).

[5]K. W. McVoy and F. J. Dyson, Phys. Rev. 106, 1360 (1957). We thank Professor C. Goebel for this reference.

[6]S. Gasiorowicz, *Elementary Particle Physics* (Wiley, New York, 1966), Chap. 12. Note that the other diagram also contributes to the helicity amplitude calculated on p. 184 of this reference.

[7]R. W. Brown, D. Sahdev, and K. O. Mikaelian, Phys. Rev. D 20, 1164 (1979).

[8]The alternative pp-collider reaction, $pp \to W\gamma X$, has been analyzed recently by G. Bunce *et al.* [in *Proceedings of the 1982 DPF Summer Study on Elementary Particle Physics and Future Facilities, Snowmass, Colorado,* edited by R. Donaldson, R. Gustafson, and F. Paige (Fermilab, Batavia, Illinois, 1982), p. 489] and H. Gordon *et al.* (*ibid.*, p. 1).

[9]C. L. Bilchak, R. Kinnunen, and J. D. Stroughair (unpublished). Also, a nice study has just been completed by J. Cortès, K. Hagiwara, and F. Herzog, Wisconsin Report No. MAD/PH/102, 1983 (unpublished).

[10]J. D. Stroughair, Ph.D. thesis, Case Western Reserve University, 1982.

[11]J. D. Bjorken and M. C. Chen, Phys. Rev. 154, 1335 (1967).

[12]K. J. F. Gaemers and G. J. Gounaris, Z. Phys. C 1, 259 (1979).

[13]The choice of $200=100\times100$ is approximately $\frac{1}{3}$ of the SPS c.m. energy (540 GeV) and also equal to the CERN LEP II c.m. energy. The choice of $600=300\times300$ is approximately $\frac{1}{3}$ of the Fermilab Tevatron II c.m. energy (2000 GeV). Of course, charged reactions such as (3.1) have no e^+e^- counterpart, corresponding to a special opportunity for proton colliders.

[14]M. Hellmund and G. Ranft, Z. Phys. C 12, 333 (1982). These authors calculate differential cross sections for the same rectangular basis used in Ref. 12.

[15]Additional numbers and remarks have been given by R. W. Brown (Ref. 4). The 80% rule is also seen there.

[16]K. O. Mikaelian, M. A. Samuel, and D. Sahdev, Phys. Rev. Lett. 43, 746 (1979). See also Ref. 7. The relationship of this zero to amplitude factorization has been developed by C. Goebel, F. Halzen, and J. P. Leveille, Phys. Rev. D 23, 2682 (1981); by Z. Dongpei, *ibid.* 22, 2265 (1980).

[17]S. J. Brodsky and R. W. Brown, Phys. Rev. Lett. 49, 966 (1982); R. W. Brown, K. L. Kowalski, and S. J. Brodsky, Phys. Rev. D 28, 624 (1983). For a recent review, see R. W. Brown, in Proceedings of the Europhysics Conference on Electroweak Effects at High Energies, Erice, 1983 (unpublished).

[18]R. W. Robinett, Phys. Rev. D 28, 1185 (1983); 28, 1192 (1983). It has also been pointed out by R. W. Brown (Ref. 4), that the $W\gamma$ rates and distributions are more sensitive to the higher-derivative interaction associated with the additional (quadrupole) parameter.

[19]The production (and decay) of $W^{\pm}$, Z^0 with a recoiling gluon in hadronic collisions has been studied in detail, for example, by P. Aurenche and J. Lindfors, Nucl. Phys. B185, 274 (1981).

[20]A discussion of $ee \to \gamma Z$ including beam-polarization effects is found in F. M. Renard, Nucl. Phys. B196, 93 (1982); and in K. I. Hikasa, Phys. Lett. 128B, 253 (1983).

[21]An early GWS calculation (massless electrons, no Higgs bosons) is by W. Allès, Ch. Boyer, and A. J. Buras, Nucl. Phys. B119, 125 (1977).

[22]R. W. Brown and K. O. Mikaelian, Phys. Rev. D 19, 922 (1979).

[23]H. Gordon *et al.*, Ref. 8.

[24]A detailed investigation of WW production and decay for proton-antiproton colliders has been carried out by J. D. Stroughair and C. L. Bilchak, Z. Phys. C (to be published).

[25]D. B. Cline, C. Rubbia, and S. van der Meer, *The Search for Intermediate Vector Bosons,* Scientific American, March (1982).

[26]T. D. Lee, P. Markstein, and C. N. Yang, Phys. Rev. Lett. 7, 429 (1961); R. W. Brown and J. Smith, Phys. Rev. D 3, 207 (1971).

[27]J. S. Bell and M. Veltman, Phys. Lett. 5, 151 (1963).

[28]R. W. Brown, R. H. Hobbs, and J. Smith, Phys. Rev. D 4, 794 (1971).

[29]R. W. Brown, L. B. Gordon, and K. O. Mikaelian, Phys. Rev. Lett. 33, 1119 (1974). See Ref. 30.

[30]L. B. Gordon and R. W. Brown, Phys. Rev. D 12, 2851 (1975). Only muon beams are considered here and in Ref. 29. The change in rates for electron beams is significant; the cross sections diverge with vanishing lepton mass.

[31]H. Uberall, Phys. Rev. 133, B444 (1964).

[32]J. Reiff, Nucl. Phys. B23, 387 (1970).

[33]An estimate of (5.3) relevant to ep colliders is found in A. N. Kamal, J. N. Ng, and H. C. Lee, Phys. Rev. D 24, 2842 (1981).

[34]A recent computation which includes all electroweak Born graphs is reported by H. Neufeld, Z. Phys. C 17, 145 (1983).

[35]F. A. Berends, R. Kleiss, P. De Causmaecker, R. Gastmans, W. Troost, and T. T. Wu, Nucl. Phys. B206, 61 (1982) and references therein.

[36]It is perhaps more the custom to define incoming $\epsilon^{\pm} \propto \epsilon^{\perp} \pm i\epsilon^{\parallel}$ for photon momentum p_1 since $(\vec{\epsilon}^{\perp}, \vec{\epsilon}^{\parallel}, \vec{p}_1)$ form a right-handed basis. The outgoing $(\epsilon^{\pm})^*$ is indeed proportional to (6.2).

[37]Reference 17 and Goebel *et al.* in Ref. 16.

[38]Compare Z times (6.6) to Eq. (4.3) of G. Passarino, Nucl. Phys. B224, 265 (1983), where the CALKUL basis is applied to all three diagrams and the p'_1 term in $\not{\epsilon}_1^{\pm}$ is not eliminated.

[39]A more general study of covariant polarization bases for vector particles and their use is in progress.

[40]The label "spinoff" suggests itself for the situation where handedness matching dominates.

[41]K. J. Kim and Y.-S. Tsai, Phys. Rev. D 7, 3710 (1973).